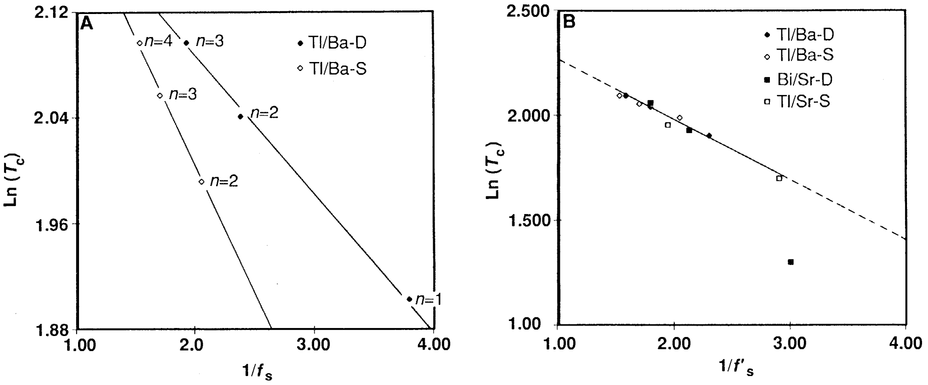

Fig. 4. (**A**) Plots of ln T_c versus $1/f_s$ for the two Tl(Ba) series with $\gamma = 1$ and $\gamma = 2$. (**B**) Master curve showing all four families scaled versus $1/f'_s$, where the "superconducting fraction" f_s is defined in Eq. 5. The symbols refer to different families: S, single B^{III} layer phase; D, double B^{III} layer phase.

that the Tl double layers play a contributing role in the superconductivity. On the other hand, the single Tl layers in a $\gamma = 1$ phase and about 50% of the Tl double layer in a $\gamma = 2$ phase formally do not contribute to T_c. We also include data for ($\gamma = 1$) Tl compounds with Sr instead of Ba ($c'_{Tl} = 0$) and ($\gamma = 2$) Bi compounds ($c'_{Bi} = 1.0$ Å). It can be seen that all data except the ($n = 1$) Bi compound fall on a common straight line that extrapolates to $T_c \approx 180$ K for the "pure" $f'_s = 1$ phase.

This extrapolation must be used with caution, since the Tl or Bi layer appears to be necessary for producing holes in the $[CuO_2]^{-2}$ layers. Thus the material with neither Tl nor Bi (or equivalent) layers is nonsuperconducting, and indeed semiconducting (*13*), even though formally $f_s = f'_s = 1$. Nevertheless, with an appropriate mix of Tl/Bi and Cu layers or by appropriate doping in the Ca^{2+} site, it may be possible to approach the extrapolated limit.

In conclusion, we have shown that T_c continues to increase with the number of Cu oxide layers for the single layer Tl cuprates at least to $n = 4$ and that the T_c data can be fitted to a common curve.

REFERENCES AND NOTES

1. C. C. Torardi *et al.*, *Science* **240**, 631 (1988).
2. M. A. Subramanian *et al.*, *Nature* **332**, 420 (1988).
3. S. S. P. Parkin *et al.*, *Phys. Rev. Lett.* **60**, 2539 (1988); *ibid.* **61**, 750 (1988).
4. R. M. Hazen, paper presented at the American Physical Society March Meeting, New Orleans, 21 to 25 March 1988; W. W. Maggs, *Eos* **69**, 236 (1988); R. Dagani, *Chem. Eng. News* **66**, 24 (16 May 1988).
5. P. Haldar, A. Roig-Janicki, S. Sridhar, B. C. Giessen, *Mater. Lett.*, in press.
6. P. Haldar *et al. J. Superconduct.* **1**, 211 (1988).
7. T. Schneider and D. Baeriswyl, in preparation.
8. P. Grant, paper presented at the Latin American Conference on High Temperature Superconductivity, Rio de Janeiro, May 1988.
9. D. E. Farrell *et al.*, *Phys. Rev. B* **36**, 4025 (1987).
10. R. H. Arendt *et al.*, in *High-Temperature Superconductivity*, M. B. Brodsky, R. C. Dynes, K. Kitazawa, H. L. Tuller, Eds. (Materials Research Society, Pittsburgh, PA, 1988), pp. 203–208.
11. K. Chen, B. Maheswaran, P. Haldar, R. S. Markiewicz, B. C. Giessen, in preparation.
12. A. Roig-Janicki, P. Haldar, B. C. Giessen, in preparation.
13. T. Siegrist, S. M. Zahurak, D. W. Murphy, R. S. Roth, *Nature* **334**, 231 (1988).
14. This work was supported by E. I. du Pont de Nemours & Company, Inc. Magnetic work was done at the Francis Bitter National Magnet Laboratory, which is supported at MIT by the National Science Foundation. N.K.J. acknowledges support by the Microelectronics and Computer Technology Corporation. We thank R. Peacetree for preparative work and J. Volf for secretarial assistance. This is publication 350 of the Barnett Institute.

22 July 1988; accepted 1 August 1988

Femtosecond Clocking of the Chemical Bond

MARK J. ROSKER, MARCOS DANTUS, AHMED H. ZEWAIL*

When a chemical bond is broken in a direct dissociation reaction, the process is so rapid that it has generally been considered instantaneous and thus unmeasurable. However, the bond does persist for times on the order of 10^{-13} seconds after the photon has been absorbed. Femtosecond (10^{-15} second) laser techniques can be used to directly clock this process, which describes the dynamics of the chemical bond. The time required to break the chemical bond in an elementary reaction has been measured and the characteristic repulsion length for the potential governing fragment separation has been obtained.

THE STRUCTURE OF THE CHEMICAL bond in molecules is now well characterized in a variety of systems. Until recently, however, the dynamics of the chemical bond have not been directly observed, because the relevant time scales involved are too rapid. For example, one might ask the question: how long does it take to break a chemical bond in the elementary reaction ABC + $h\nu \rightarrow$ A + BC? Two fundamental processes are involved in this reaction. The first, which is virtually instantaneous, is the transition of ABC from its ground (bound) potential energy surface (PES) to an excited (dissociative) PES. The second process, the so-called half-collision, involves the subsequent time evolution of the molecule on this dissociative PES. This evolution must lead to the spatial separation of the fragments; when the fragments no longer interact, the chemical bond is broken.

The terminal velocities of separation of the fragments for such reactions are typically ~1 km s^{-1} (=0.01 Å fs^{-1}). If the bond is considered to be broken when the fragments are a few times their equilibrium bond length apart (typically several angstroms), then the time required to break the bond must be of the order of a few hundred femtoseconds. Recent advances in ultrafast laser spectroscopy of chemical reactions (*1–5*) have allowed the observation of chemical bond dynamics on this time scale. We report the direct clocking measurement of bond-breaking time in the elementary reaction ICN + $h\nu \rightarrow$ I + CN.

The dissociation reaction of ICN on the repulsive surface passes through transition-state configurations,

$$ICN^* \rightarrow [I \cdots CN]^{\ddagger *} \rightarrow I + CN$$

where the bond stretches from the initial value at R_0 to "infinite" separation, that is, when the I and CN fragments are sufficiently separated so as to no longer interact. Real-time observations of these transition states ($[I \cdots CN]^{\ddagger *}$) have been made with femtosecond transition-state spectroscopy (FTS), a technique for viewing the fragments en route to products (*2*). However, the absolute clocking of these transition states and of the final states (free fragments) was not established, since the exact zero-of-time was not determined. To measure the actual time for bond breaking and to obtain informa-

---

Arthur Amos Noyes Laboratory of Chemical Physics, California Institute of Technology, Pasadena, CA 91125.

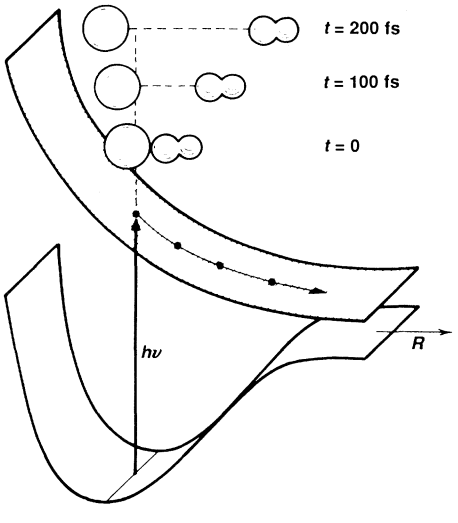

Fig. 1. A cartoon illustrating the experiment. A simple (slice through) one-dimensional picture, with no angular dependence, is considered for the sake of clarity. The actual surfaces are discussed in the text. At time $\tau = 0$, the laser pulse promotes the molecule to the upper potential energy surface. For $0 < \tau < \tau_{1/2}$, the bond stretches. By $\tau = \tau_{1/2}$, the bond is essentially broken.

tion on the PES governing the I and CN fragments internuclear separation R, we have now obtained the zero-of-time. We find that for excitation with femtosecond pulses, the bond between I and CN breaks 205 ± 30 fs after photoexcitation at 306 nm. At the terminal velocity of recoil, this corresponds to 5.3 Å of increased separation of the fragments. This value is essentially an upper bound, since the velocity of recoil begins at zero and changes with distance, as discussed below.

The experiment is cartooned in Fig. 1. A femtosecond optical pulse is used to initiate the reaction by excitation of gas-phase ICN at 306 nm. This corresponds to 6×10^3 cm^{-1} of translational energy (*6*) above the bond dissociation energy (~74 kcal mol^{-1}), which leads to a terminal recoil velocity of $v_t = 2.6 \times 10^5$ cm s^{-1} (= 0.026 Å fs^{-1}). The pump pulse (*7–11*) sets the exact zero-of-time for the dissociation. The second optical pulse (near 388 nm) probes the CN fragment as a function of the delay time τ between the two pulses. The duration of the bond breaking is observed as a delay between the zero-of-time and the appearance of absorption by the probe, as measured by the associated laser-induced fluorescence (LIF).

A Michelson interferometer arrangement was used to delay the probe pulse relative to the pump pulse, and the delay time was determined by a precision actuator with submicrometer resolution (a crucial consideration, as 100 fs corresponds to a spatial separation of only 30 μm). The pump and probe beams, with proper attenuation and parallel or perpendicular polarization, were collinearly recombined and focused into the reaction chamber. The LIF of the CN was collected perpendicular to the direction of the pump-probe pulses. For every data set, we characterized the transients by taking: (i) the cross-correlation of the pulses, (ii) the frequency spectrum of the pulses, and (iii) the zero-of-time and the overall temporal response function of our apparatus.

The zero-of-time was determined by using the following idea: in situ, the ICN was evacuated from the chamber and replaced by *N*,*N*-diethylaniline (DEA). The experiment was repeated as before, except that the resonance-enhanced multiphoton-ionization signal (pump photon + probe photon) was measured rather than the LIF. This photoionization experiment gave the integral of the response function of the pump and probe (*1*), as we verified by obtaining the cross-correlation of the pump and probe using nonlinear (infrared) difference frequency generation. The zero-of-time was set when the photoionization signal reached one-half its limiting value (*12, 13*). Note that these measurements were made in situ, with no realignment of the optical beams or repositioning of the cell, either of which could have significantly shifted the $\tau = 0$. Care was taken to insure that pulses were chirp-free (transform limited, that is, $\Delta\nu\ \Delta t$ = 0.3 to 0.5), but data with pulses of larger $\Delta\nu\ \Delta t$ have also been obtained.

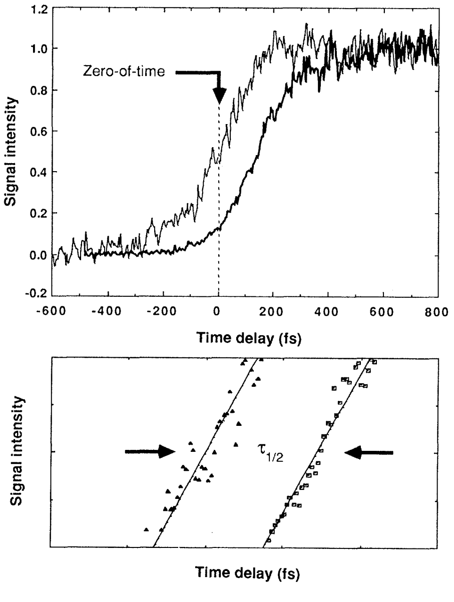

Fig. 2. Typical experimental results. The heavy line is the measured ICN transient, and the thin line is the reference $\tau = 0$ transient. The figure at the bottom shows a magnified view near $\tau = 0$. The observed delay for transform-limited pulses (see text) is 205 ± 30 fs. The error here is estimated from the scatter observed in several measurements.

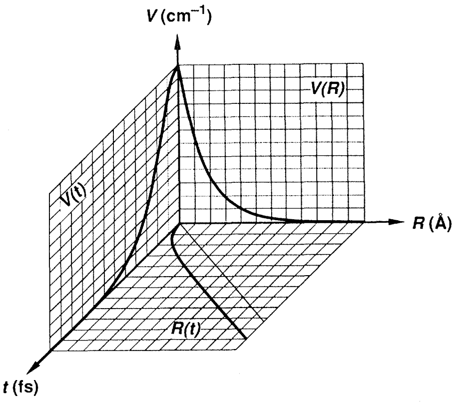

Fig. 3. A potential energy surface as a function of the parameter t (time), with 25 fs per division, and as a function of the parameter R (internuclear distance), with 0.5 Å per division. An exponential shape is assumed, and the initial potential energy at $t = 0$ (and $R = 0$) is 6000 cm^{-1} (17.2 kcal mol^{-1} above dissociation). Note that the difference between $R(t)$ and R at the terminal velocity (the straight line) approaches a constant at long time; this difference represents the invariant τ_d defined in the text.

The main experimental result is shown in Fig. 2. The LIF signal was delayed from the photoionization trace by $\tau_{1/2}$ = 205 ± 30 fs. This result was highly repeatable for the transform-limited femtosecond pulses used. We performed the experiments for different pump polarizations, keeping the probe polarization parallel to the detection axis, and obtained similar $\tau_{1/2}$ values (*14–16*). The value of $\tau_{1/2}$ should be a fundamental property of the chemical bond; it is determined by the PES.

To relate $\tau_{1/2}$ to a dissociation time and to the characteristics of the PES, we consider for repulsion between the I and the CN fragments in their ground states a potential of the form given by Goldfield *et al.* (*16*):

$$V(R) = V_0 \exp(-R/L_1) f(\theta, R)$$

where L_1 is the repulsion length parameter, V_0 is a constant, and $f(\theta, R)$ describes the angular part, which we shall ignore for now. The classical equation of motion for this system can be integrated to give explicitly the internuclear separation of the fragments as a function of time, $R(t)$, and the corresponding potential as a function of time, $V(t)$.

We then ask, what defines a dissociation time? If it were defined as the time for the two fragments to reach a separation at which their interaction energy is negligible, the dissociation time would depend on the sensitivity with which the energy can be measured; an infinite time is required to reach infinite separation. A more invariant definition is obtained as follows. Consider the difference between the time taken for the fragments to separate from R_0, the separation at the instant of photoexcitation, to R (as they travel along the actual potential) minus the time that would be required had the fragments traveled at the terminal velocity. Then τ_d is defined as the limit of this difference as $R \rightarrow \infty$. For the potential described above (with no anisotropy), one obtains (*17*) $\tau_d = (L_1/v_t) \ln 4$. Although well defined, this τ_d is obtainable only from a hypothetical experiment requiring the measurement of minute differences in long arrival times (see Fig. 3).

A more useful description of bond breaking has been recently developed by Bersohn and Zewail (*17*), who considered the time dependence of fragment separation and the absorption by fragments during this separation. When the fragments develop to be spectroscopically free, the absorption achieves a maximum. Dissociation can be defined as the time delay when the midpoint of the absorption is reached:

$$\tau_{1/2} = (L_1/v_t) \ln (4E/\gamma)$$

Here, γ is the half-width of the energy distribution of the probe pulse, and E is the energy available above dissociation ($E > \gamma$). An important observation is contained within this analysis: the probe spectral width determines a "window" for which the free CN fluorescence is viewed, and so affects $\tau_{1/2}$ (*18*). Since we have both γ (40 cm^{-1}) and E, the above expression yields for the repulsion length parameter $L_1 = 0.8$ Å for the exponential potential discussed above. Similar procedures can be used to calculate length parameters of other potential shapes, for example, R^{-n}. In Fig. 3, the derived $V(R)$, $V(t)$, and $R(t)$ are all shown in a construction that illustrates the "trajectory" for dissociation through space-time, and that provides the time and distance scales involved. According to the above analysis, the potential falls to $1/e$ of its initial value in 0.8 Å, but the length required to break the bond may be several times this value. For the potential to drop to the value of γ, the bond is broken at 2.8 Å, which is to be contrasted with the value of 5.3 Å obtained earlier when the fragments were presumed to be moving at their terminal velocity throughout.

There are several points to be made regarding this reaction. First, the PES of ICN dissociation is more complex than the one illustrated here, because there are two channels [with possible crossing (*16*)] for dissociation involving the production of iodine either in its ground or its excited spin-orbit states. However, our available energy is just below the excited I* state channel, and it is known experimentally that at our excitation wavelength, the reaction is to the ground state channel, which correlates with a bent state. The measurements reported here clock the dynamics of I–CN recoil and the development of free CN. As pointed out by Zare and co-workers (*16*), the dynamics that produce rotational excitation (bending) could be on a shorter time scale, and time-resolved alignment experiments would aid us in resolving this bending dynamics. At our wavelength of dissociation, the product rotational-state distribution of the nascent CN was explained (*19*) by nearest-neighbor repulsion effects exclusively. This explanation is consistent with the picture here of repulsion between the carbon and the iodine. Second, the absorption measurement depends also on the characteristic of the upper state (I + CN*) potential. However, in the asymptotic limit ($R \rightarrow \infty$), $\tau_{1/2}$ is described for the potential discussed by the formula given above (*20, 21*). Finally, we assumed here the repulsive potential of Goldfield *et al.* (*16*), but there exists a method to invert the data to give the shape of the PES and to account for the attractive terms in the potential (*22*).

With femtosecond pulses it is now possible to clock chemical reactions as they occur. Based on a classical mechanical model, we can describe the important physics relevant to these clocking experiments. This description is also consistent with recent quantum mechanical simulations of the experiment by Williams and Imre (*23*). In general, the precision to which the time delay (clocking) can be measured is determined by the experimental signal-to-noise ratio (eventually, one will be limited by the accuracy by which a molecule like DEA gives the $t = 0$ calibration), whereas the temporal pulse width influences observations relating to the distribution of molecules. Increasing the temporal resolution further may lead to additional information on the dispersion of molecules as they travel on the PES. Furthermore, trapping phenomenon like the one observed in the reaction of salt molecules may also be observed (*3, 4*). These real-time femtochemistry (*24*) experiments promise to provide a new window on the dynamics of the chemical bond, with sub-angstrom resolution, in many other chemical reactions.

REFERENCES AND NOTES

1. N. F. Scherer, J. L. Knee, D. D. Smith, A. H. Zewail, *J. Phys. Chem.* **89**, 5141, (1985).
2. M. Dantus, M. J. Rosker, A. H. Zewail, *J. Chem. Phys.* **87**, 2395 (1987).
3. T. S. Rose, M. J. Rosker, A. H. Zewail, *ibid.* **88**, 6672 (1988).
4. M. J. Rosker, T. S. Rose, A. H. Zewail, *Chem. Phys. Lett.* **146**, 175 (1988).
5. J. L. Knee and A. H. Zewail, *Spectroscopy* **3**, 44 (1988).
6. This value equals the total energy minus the bond energy. We also subtract the average rotational energy of the nascent CN fragment.
7. The femtosecond laser pulses were generated by a home-built, colliding-pulse, mode-locked ring dye laser following the design of Shank and colleagues (*8*). The laser produced pulses as short as 40 fs near 620 nm. These pulses were amplified to peak powers of 5 GW at a 20-Hz repetition rate by a yttrium-aluminum-garnet–pumped (532 nm), four-stage, pulsed dye amplifier (*9*). Pulse broadening due to group velocity dispersion in the amplifier was corrected by the suitable arrangement (*10*) of four high-index SF10 glass prisms (*11*) to yield pulses as short as 60 fs with 300-μJ energy. This wave train was split in half, and the pump at 306 nm was produced by second-harmonic generation of one arm of this light in a nonlinear crystal. For the probe arm, light at 388 nm was generated by mixing the femtosecond pulses with residual 1.06-μm radiation from the pump laser in a second nonlinear crystal.
8. R. L. Fork *et al.*, *Appl. Phys. Lett.* **38**, 671 (1981); J. A. Valdmanis, R. L. Fork, J. P. Gordon, *Opt. Lett.* **10**, 131 (1985).
9. R. L. Fork, C. V. Shank, R. T. Yen, *Appl. Phys. Lett.* **41**, 223 (1982).
10. R. L. Fork *et al.*, *Opt. Lett.* **9**, 150 (1984).
11. J. D. Kafka and T. Baer, paper presented at CLEO '85, Conference on Lasers and Electro-Optics, Baltimore, May 1985.
12. DEA was chosen for the calibration of the $t = 0$ because the intermediate lifetime (aniline type) of the state reached by the pump pulse is long-lived. Hence the signal will rise "instantaneously" with our pulse and will reach a plateau at long times, as observed experimentally. By instantaneous, we mean that it is as fast as any electronic transition response [see (*13*)].
13. M. J. Rosker, M. Dantus, A. H. Zewail, unpublished results.
14. Similar experiments have been done away from the "free CN" absorption to the red (and also to the blue) of 388 nm to study the alignment and to clock the earlier buildup and decay of the transition states observed previously (*2*); these results are consistent with the results presented here (*13*). When these experiments are completed at the different wavelengths, more should be learned about coherence (*15*) during fragmentation, the angular dependence and curve crossing (*16*), and (if it exists) trapping (*3, 4*) on the PES.
15. P. M. Felker and A. H. Zewail, *J. Chem. Phys.* **86**, 2460 (1987); J. S. Baskin *et al.*, *ibid.* p. 2483; J. S. Baskin *et al.*, *ibid.* **85**, 7488 (1986).
16. M. A. O'Halloran, H. Joswig, R. N. Zare, *ibid.* **87**, 303 (1987), and references therein; E. M. Goldfield, P. L. Houston, G. S. Ezra, *ibid.* **84**, 3120 (1986), and references therein.
17. R. Bersohn and A. H. Zewail, *Ber. Bunsenges. Phys. Chem.* **92**, 373 (1988).
18. As the spectral bandwidth is reduced, we would anticipate that $\tau_{1/2}$ would increase, since the potential is viewed at longer R. This expectation is consistent with the results of (*1*), where $\tau_{1/2}$ was estimated to be longer (~600 fs for the full rise), as discussed in (*13*).
19. For recent discussion of dissociation at this wavelength, see C. H. Dugan and D. Anthony, *J. Phys. Chem.* **91**, 3929 (1987), and references therein.
20. As shown in (*17*) for repulsive surfaces, if the upper surface has different L values from the lower surface on which the dynamics is taking place, then this does not influence the dynamics when probing free CN as it would if probing the PES at shorter R. It is assumed that the upper surface will either reach its asymptotic level more quickly than the lower surface or that its total change in energy will be less than that of the lower surface (*21*).
21. See H. J. Foth, J. C. Polanyi, H. H. Telle, *J. Phys. Chem.* **86**, 5027 (1982), and references therein.
22. R. B. Bernstein and A. H. Zewail, unpublished results.
23. S. Williams and D. Imre, *J. Phys. Chem.*, in press.
24. See (*5*), and references therein; R. B. Bernstein and A. H. Zewail, *Kagaku Kogyo* **41**, 108 (1988).

25. We thank R. Zare, R. Dixon, J. Simons, and K. Wilson for very enlightening discussions. Supported by the AFOSR grant 87-0071. A.H.Z. is a John Simon Guggenheim Foundation Fellowship.

6 June 1988; accepted 6 July 1988